Journal of Low Temperature Physics, Vol. 54, Nos. 1/2, 1984

Transport Properties in ^{3}He–^{4}He Mixtures Near the Superfluid Transition*

David Gestrich, Ron Walsworth, and Horst Meyer

Department of Physics, Duke University, Durham, North Carolina

(Received May 13, 1983)

We report measurements of the temperature, density, and concentration gradients in ^{3}He–^{4}He mixtures, induced by a vertical heat flux. The flat horizontal cell included two superposed capacitors and the density was determined by means of the dielectric constant method. The experiments were carried out on mixtures with mole fractions $X_3 = 0.37$, 0.15, and 0.05 at saturated vapor pressure, with special emphasis on the region near the superfluid transition. Our measurements under steady-state conditions give the conductivity κ, the thermal diffusion ratio k_T, and the coefficient of thermal expansion. We describe the singular behavior of these quantities in the neighborhood of $T_\lambda(X)$. In the superfluid phase, we test with fair success a relation by Khalatnikov between grad X/grad T and several static properties. From the relaxation times needed to attain steady-state conditions, and in combination with measured static and transport properties, we obtain in the normal phase the mass diffusion D, which diverges strongly as T_λ is approached. In the superfluid phase, we test successfully a scaled relation that results from the solution of Khalatnikov's hydrodynamic equations. From our data the dispersion relations for scattered light are calculated: Γ_0/q^2 in both the normal and the superfluid phases and Γ_2/q^2 in the normal phase.

1. INTRODUCTION

This paper is the second in a systematic study of transport properties for ^{3}He–^{4}He mixtures at saturated vapor pressure along the superfluid transition critical line. The properties to be described are the thermal conductivity κ, the thermal diffusion ratio k_T, and the mass diffusion coefficient D. The first paper[1] dealt with the region near the tricritical point and covered mixtures with ^{3}He mole fractions $0.51 \leq X \leq 0.72$. The present paper extends this range to $X = 0.05$ with the study of three mixtures.

*Research supported by NSF grant DMR 8024056.

0022-2291/84/0100-0037$03.50/0 © 1984 Plenum Publishing Corporation

A third paper[2] will deal with very dilute mixtures, including pure ^{4}He, where only thermal conductivity measurements will be presented.

There has been in recent years some theoretical interest in mixtures[3–5] and most recently a new attack[6,7] has been made on the problem. Both the asymptotic power law behavior for κ in pure ^{4}He[8,9] and the temperature range for the asymptotic critical transport properties in dilute ^{3}He–^{4}He mixtures above T_λ are very difficult to reach by experiments. The recent theoretical advances consist in the calculation of the crossover functions between the critical scaling and the regular or "background" behavior. A discussion of the predictions is presented in detail, together with our results, in two recent theoretical papers,[6,7] and therefore it will be omitted here.

Also, because the apparatus and the experimental techniques have been described in some detail in Ref. 1, they will only be briefly reviewed here. In Ref. 1 a review of the hydrodynamic transport equations and certain predictions by the Khalatnikov theory[11] in the superfluid phase have been given, to which we refer the reader. Therefore, the paper consists mainly of a presentation of the experimental results and a comparison with previous measurements and predictions, where available.

The paper is organized as follows: In Section 2, we give a brief review of the transport property relations, the apparatus, and the method of data analysis, with emphasis on aspects that were not discussed in Ref. 1, because they were less relevant for concentrated mixtures. In Section 3, the data for steady-state measurements of κ and k_T are presented and compared with previous experiments and theory. Section 4 deals with the analysis of the transient measurements that provide the characteristic relaxation times. From these the mass diffusion coefficient D is derived for the normal phase, while for the superfluid phase a scaled relation derived from hydrodynamic equations is compared with experiment.

2. REVIEW OF THEORY AND EXPERIMENTAL PROCEDURE

2.1. Transport Property Relations

The transport properties κ and k_T have been measured in an approximately one-dimensional geometry under steady-state conditions as described previously.[1] In the normal phase these conditions imply a zero ^{3}He mass flux, $i = 0$, leading to

$$\kappa = -\mathbf{q}/\nabla T \tag{1a}$$

$$k_T = -T\,\nabla c/\nabla T \tag{1b}$$

where c is the mass concentration of ^{3}He.

In the superfluid phase we use the results of Khalatnikov's theory,[11] but we cannot separately determine k_T. If we define as $\mathbf{v}_n$ the velocity of the normal component of ^{4}He, then in the steady state the total ^{3}He mass flux $\mathbf{i}+c\mathbf{v}_n$ will be zero and one has

$$\nabla c=-(k_T/T)\nabla T+(c/D)\mathbf{V}_n \tag{2}$$

By making the additional assumption that dissipative terms arising from viscosity are small, one has $\nabla\mu=0$ and also a zero pressure gradient, $\nabla P=0$. This condition leads to the relation

$$\frac{\nabla c}{\nabla T}=c\left(\frac{\partial c}{\partial\mu}\right)_{T,P}\left[\frac{\partial}{\partial c}\left(\frac{\sigma}{c}\right)\right]_{P,T} \tag{3}$$

where σ is the entropy per unit mass [Ref. 11, Eq. (24-54)], and $\mu=\mu_3/M_3-\mu_4/M_4$ is the difference between the chemical potentials per gram of mixture. By analogy with the normal fluid, we define for convenience

$$k_T^*\equiv -T\nabla c/\nabla T \qquad \text{(superfluid)} \tag{4}$$

which is the quantity determined from the experiment.

In the superfluid the conductivity measured in the steady state is denoted by κ_{eff}, and it differs from κ because it includes the energy flux carried along by nondiffusive mass currents [Eq. (24-58) of Ref. 11], and is written as

$$\kappa_{\text{eff}}=\kappa+\rho DT\left(\frac{\partial c}{\partial\mu}\right)_{P,T}\left[c\frac{\partial}{\partial c}\left(\frac{\sigma}{c}\right)_{P,T}+\frac{k_T}{T}\left(\frac{\partial\mu}{\partial c}\right)_{P,T}\right]^2 \tag{5}$$

The conversion from the units used in the experiments (mole fraction X of ^{3}He, chemical potential difference Δ, entropy S, and volume V, all per mole) to those used in the theory (c, μ, σ, and ρ) has been discussed elsewhere.[12,1] For convenience, we summarize the expressions, which are

$$c=XM_3/\bar{M}$$

with the average molar mass $\bar{M}$ given by

$$\bar{M}=XM_3+(1-X)M_4 \tag{6}$$

and

$$\left(\frac{\partial X}{\partial\Delta}\right)_{T,P}=\frac{\bar{M}^3}{M_3^2M_4^2}\left(\frac{\partial c}{\partial\mu}\right)_{T,P} \tag{7}$$

In the normal phase one has

$$\frac{k_T}{T}=-\frac{\nabla X}{\nabla T}\frac{M_3M_4}{\bar{M}^2} \tag{8}$$

and in the superfluid

$$\frac{k_T^*}{T} = -\frac{\nabla X}{\nabla T}\frac{M_3 M_4}{\bar{M}^2} = -\frac{M_3 M_4}{\bar{M}^2} X \left(\frac{\partial X}{\partial \Delta}\right)_{T,P} \left[\frac{\partial (S/X)}{\partial X}\right]_{T,P} \tag{9}$$

In the limit of very dilute mixtures, this expression becomes[11]

$$\frac{k_T^*}{T} = \frac{M_3 M_4}{\bar{M}^2}\frac{X}{T}\left(1 + \frac{S_0 M_4}{RX}\right) \tag{10}$$

where S_0 is the molar entropy of liquid ^{4}He and R is the gas constant. Inserting the value $S_0(T_\lambda) = 6.24$ J/mole K,[12] we obtain

$$\lim_{X \to 0} k_T^*(T) = 0.57 \tag{11}$$

2.2. The Apparatus

The experiment consists in measuring the vertical temperature and density gradients induced by a vertical heat flow across the fluid layer. The sample cell, the top of which is in thermal contact with a temperature-regulated platform, consists of two flat horizontal copper end pieces of 1.9 cm diameter, separated by a stainless steel spacer 0.28 cm long. To each of these copper plates is attached a capacitor made of two thin, perforated stainless steel disks. The capacitors measure the dielectric constant and hence the molar volume V at the top and bottom of the cell. Two matched Ge resistors embedded in the copper pieces measure the temperature gradients. The temperature resolution was about 0.3 μK and the control of the platform was of the order of 1 μK. The resolution and stability of the ratio transformer capacitance bridge were such that dielectric constant changes of $\delta\varepsilon = 1 \times 10^{-8}$ or better could be seen. Because over most of the investigated temperature region the coefficient of thermal expansion $\alpha_{p,X}$ is negative, the heat flux is directed upward so as to reduce the possibility of convection. In the region above T_λ where $\alpha_{p,X}$ is positive, careful checks were made to keep the heat flux below the critical value where convection appears. This unfortunately limited the accuracy of the k_T measurements at temperatures well above T_λ, where k_T had become very small. However, in another study of transport properties of mixtures in the region of the liquid–vapor critical line, where $\alpha_{p,X}$ is always positive, this same cell has been used with the heat flowing downward, and the measurements were extended to temperatures below 2 K. The results will be discussed elsewhere[13] and compared with the present ones.

For the thermal conductivity measurements, where the ratio of the cross section $\mathcal{A}$ to the distance d between the parallel copper plates must

be well defined and the path unobstructed, the geometry of our cell is obviously not ideal. The insertion of the perforated capacitor complicates the heat flow path and also the mass flow during the observation of the transients. Thus it will not be unexpected if an effective ratio $(\mathscr{A}/d)_{\text{eff}}$ rather than the nominal one should enter into the diffusive transport equations. Also, an effective distance might have to be used in calculating the mass diffusion and characteristic parameters from transient experiments (see Section 4). Yet the choice of the nominal ratio $(\mathscr{A}/d)_{\text{nom}} = (\mathscr{A}/d)_{\text{eff}}$ gave for the control experiment with ^{3}He a surprisingly good agreement with other experiments (see Appendix A).

In Appendix B we present a simple derivation of the measured changes δV in the molar volume between the top and the bottom of the cell in the presence of a temperature difference δT. We then obtain the ratio grad V/grad T in terms of geometrical parameters in the cell. The corresponding mole fraction change δX is derived via the relation

$$\delta V = \left(\frac{\partial V}{\partial T}\right)_{X,P} \delta T + \left(\frac{\partial V}{\partial X}\right)_{T,P} \delta X \tag{12}$$

which gives

$$\frac{\nabla X}{\nabla T} = \left(\frac{\partial X}{\partial V}\right)_{T,P} \left[\frac{\nabla V}{\nabla T} - \left(\frac{\partial V}{\partial T}\right)_{P,X}\right] \tag{13}$$

In the previously investigated[1] concentrated mixtures ($0.51 \leq X \leq 0.72$) the first term on the right-hand side is much larger than the second one, and also $(\partial V/\partial X)_{T,P}$ is a reasonably smooth function of T. However, for lower ^{3}He concentrations the situation is more complicated because the singularity of $(\partial V/\partial T)_{P,X}$ near T_λ becomes more pronounced as X decreases. This leads to an enhanced singularity for $(\partial V/\partial X)_{P,T}$ as well, as can be seen from the relation

$$\left(\frac{\partial V}{\partial X}\right)_{T,P} = \left(\frac{dV}{dX}\right)_t - \left(\frac{dT}{dX}\right)_t \left(\frac{\partial V}{\partial T}\right)_{X,P} \tag{14}$$

where $(\cdots)_t$ is a differentiation along a path at fixed $t = T - T_\lambda$ parallel to the lambda line. We have measured over small temperature increments the average density in the cell taken from the bottom and top capacitors in the absence of heat flux and we have obtained $(\partial V/\partial T)_{P,X}$ by differentiation. The singularity of $(\partial V/\partial X)_{T,P}$ was then obtained using parameters along the lambda line as presented by Ahlers.[12] Because $(\partial V/\partial T)_{P,X}$ tends to cancel grad V/grad T in Eq. (13), the absolute value of k_T becomes more sensitive to systematic errors in the measured quantities as X is decreased. From our experience we feel that it will be difficult, using the present

technique, to measure k_T with sufficient accuracy as ^{3}He concentrations become smaller than, say, 0.03. Near the superfluid transition, where the temperature changes δT between top and bottom are kept as low as 15 μK, the scatter in δX and in δT could reach about 15% and 5%, respectively. To a major extent, the scatter in these experiments at the smallest gradients is caused by the long relaxation times of the system, which permit drifts in the temperature and capacitance measurements to become significant.

A favorable feature of the mixtures with $X \leqslant 0.51$ is the absence of the onset of a superfluid film flow[1] at a temperature above the bulk transition $T_\lambda(X)$. The analysis of the thermal transport properties is then considerably simplified.

3. RESULTS: STEADY-STATE MEASUREMENTS

Since they assume such a considerable importance in the data analysis, we present first our results for the thermal expansion coefficient and $(\partial V/\partial X)_{T,P}$, then compare these with other reported values. Second, we present the data for the thermal conductivity and k_T and compare them with previous experimental work.[14–19] A technical report is in preparation with a tabulation of these results.

3.1. Thermal Expansion Coefficient

Previous molar volume measurements in mixtures under saturated vapor pressure include those by Kierstead[20] and by Kakizaki and Sato.[21] Those by Kierstead,[20] made at concentration intervals of about $\delta X \simeq 0.1$, cover the wide temperature range between the phase separation curve below $T_t = 0.87$ K and above the superfluid transition line $T_\lambda(X)$. There was no detailed investigation of the critical region. By contrast, the measurements in Ref. 21 focus on the range $|T - T_\lambda| \leqslant 0.03$ K on both sides of the transition. Our own measurements extended over the range expected to cover the transport properties. The upper temperature limit went beyond that of the molar volume minimum until k_T became very small and the scatter correspondingly large. The lower temperature limit extended about 0.5 K below T_λ.

In Fig. 1 we present the data for $(\partial V/\partial T)_{X,P}$ for the three mixtures as a function of the reduced temperature $\varepsilon = (T - T_\lambda)/T_\lambda$. The most precise location of T_λ was from the sharp break of the κ and k_T data at the transition (see Section 3, Figs. 3 and 5) and this determination was found to be consistent with the extremum in $(\partial V/\partial T)_{P,X}$. In Table I we present a list of the mixtures, transition temperatures, and parameters used in the thermodynamic calculations. Only for one mixture, $X = 0.154$, can our data

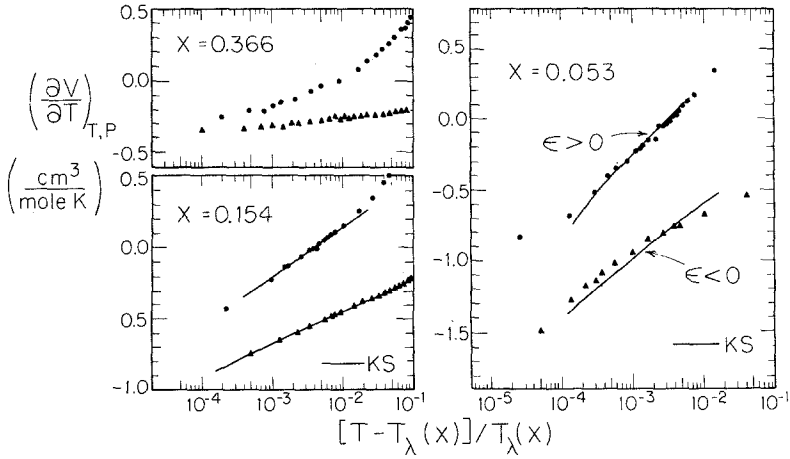


Fig. 1. The volume change with temperature $(\partial V/\partial T)_{X,P}$ for three diluted mixtures versus the reduced temperature. The solid lines represent the data of Kakizaki and Sato,[21] obtained as explained in the text.

be directly compared with those of Ref. 21 and this is shown in Fig. 1 by solid lines representing the Tohoku results. Our mixture with $X = 0.053$ can be compared with an interpolation of the results[21] between $X = 0.10$ and 0.038. The agreement appears reasonable.

3.2. The Derivative $(\partial V/\partial X)_{T,P}$

We have obtained this quantity in two ways. First, for the region outside the critical range we differentiated at constant T both our own volume measurements and those from Ref. 20. Second, for the region close to the transition we used Eq. (14). Here we first determined the dependence of $(\partial X/\partial V)_t$ on t for a given mixture, again from the differentiation of density data. Furthermore, we found that $(\partial X/\partial T)_t \approx (\partial X/\partial T)_{t=0}$. The results from

TABLE I

Parameters Along the Lambda Line Used in the Analysis of the ^{3}He–^{4}He Mixtures

X	T_λ, K	V_λ, cm^3/mole	dT_λ/dX K	dV_λ/dX, cm^3/mole	S_λ, J/mole K	dS_λ/dX, J/mole K
0.510	1.2695	31.790	−2.309	9.407	12.04	−4.0
0.366	1.5791	30.399	−1.965	8.789	12.12	3.0
0.154	1.9433	28.516	−1.555	7.778	10.29	14.4
0.053	2.0967	27.766	−1.453	7.308	8.29	26.6

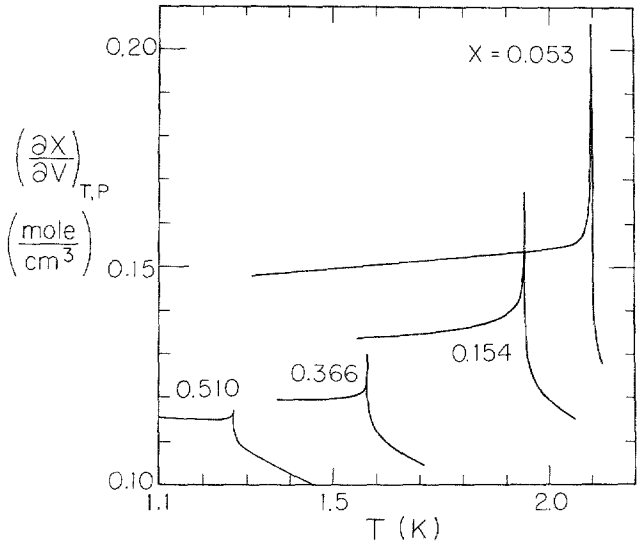


Fig. 2. Display of the calculated coefficient $(\partial X/\partial V)_{T,P}$ showing the singularities near T_λ.

the two ranges were internally consistent within about 5%, and are shown in Fig. 2. We have also recalculated $(\partial X/\partial V)_{T,P}$ for the mixture $X = 0.51$ investigated in Ref. 1, and have reanalyzed all the transport data so that a comparison could be made with the more dilute mixtures. The divergence of $(\partial X/\partial V)_{T,P}$ becomes increasingly sharper as X decreases.

3.3. The Thermal Conductivity

Measurements from two laboratories[14,17] have shown that the conductivity for ^{3}He–^{4}He mixtures is singular but finite at T_λ. The first investigation was made by Ahlers[14] on an $X = 0.15$ mixture at saturated vapor pressure. A study on a number of mixtures with $X \leq 0.3$ was made by Tanaka and Ikushima.[17] It was found that upon approaching T_λ in the normal phase κ strongly increased, and there was a sharp break in the slope $d\kappa/dT$ at T_λ. In the superfluid phase κ_{eff} decreased slowly with T. Ahlers[14] discussed in detail how the effect of the concentration gradient that accompanies the temperature gradient leads to a two-phase region close to the superfluid transition. The heat flux Q he used in his cell of 1 mm height produced a temperature difference of 400 μK between the top and bottom, and an estimated two-phase region 200 μK wide. Tanaka and Ikushima,[17] working

with cells of 0.5 and 1.3 mm height, did not specify the heat flux they used. As mentioned previously, our own heat fluxes were adjusted to produce temperature differences as low as 15 μK, and for each temperature several values were used to verify the independence of κ on Q. Hence, in our situation the two-phase region was considerably smaller than in Ahlers' experiment[14] for the same mixture $X = 0.15$. However, the scatter of the data was on the order of several percent for the lowest heat inputs, which is larger than that from Ahlers' data. In Fig. 3a we show a plot of κ data

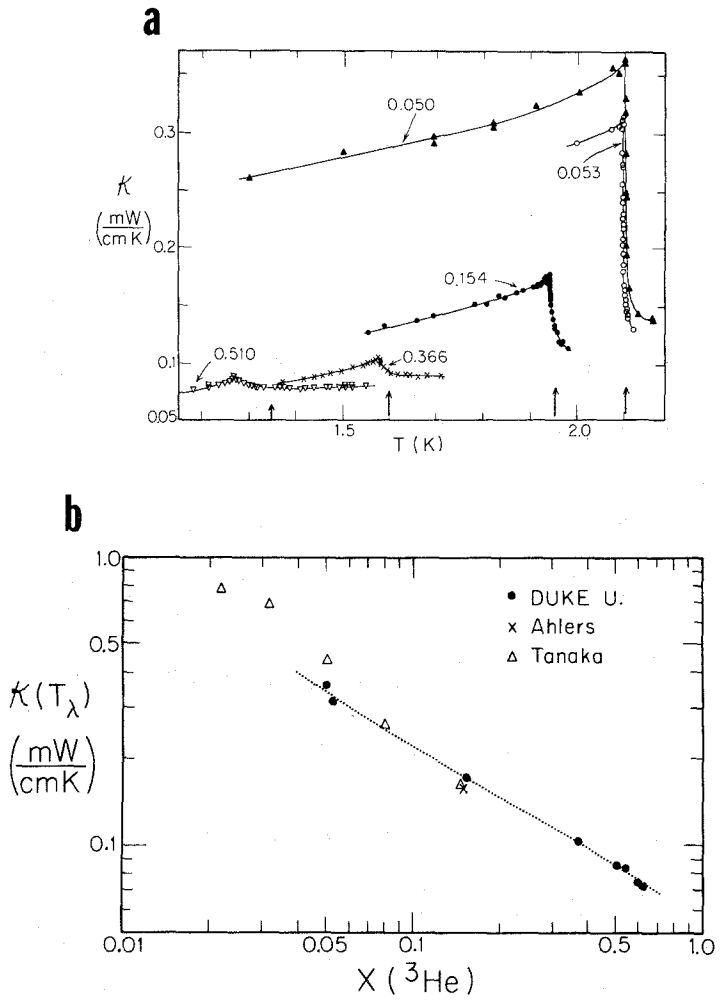


Fig. 3. Display of the thermal conductivity for four mixtures.

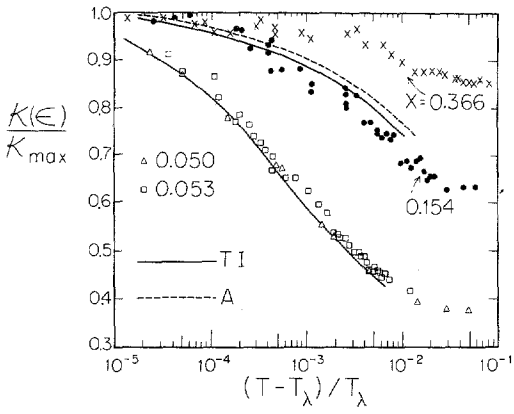


Fig. 4. Reduced representation κ/κ_{max} data versus the reduced temperature, and comparison with the data by Ahlers[14] (dashed line) and Tanaka and Ikushima[16] (solid line).

for five mixtures, which brings out the relative magnitudes and singularities of κ. The mixture $X = 0.050$ was measured with a straight thermal conductivity cell with a height of 1.2 mm during the course of experiments with still more diluted mixtures.[2] In Fig. 3b we compare the maximum conductivity for mixtures investigated in this laboratory (present data and Ref. 1) with those by Ahlers[14] and Tanaka and Ikushima.[17] For the most dilute mixtures this conductivity was obtained from extrapolating to T_λ the data in the superfluid phase, where their temperature dependence is much weaker than for $T > T_\lambda$.

For further data comparison it is useful to present the results in reduced units above T_λ as shown in Fig. 4. We normalize the data to the peak value denoted by κ_{max}, which is measured for $\varepsilon \lesssim 5 \times 10^{-6}$ but does not necessarily correspond to the value at T_λ, since effects from the presence of two phases and limited resolution might well prevent us from detecting the true maximum height. We note a good agreement with previous results[14,17] on mixtures where comparison could be made.

3.4. Thermal Diffusion Ratio

Previous work includes the measurements of Lucas and Tyler[15] by means of an NMR technique, which first showed a weak singularity of k_T for a mixture with $X = 0.15$, but did not give absolute values. Tanaka and Ikushima[18,19] used a capacitor arrangement very similar to the one in our past[1] and present work and also found a weak divergence of k_T with a peak at T_λ. Their results were independent of concentration over their

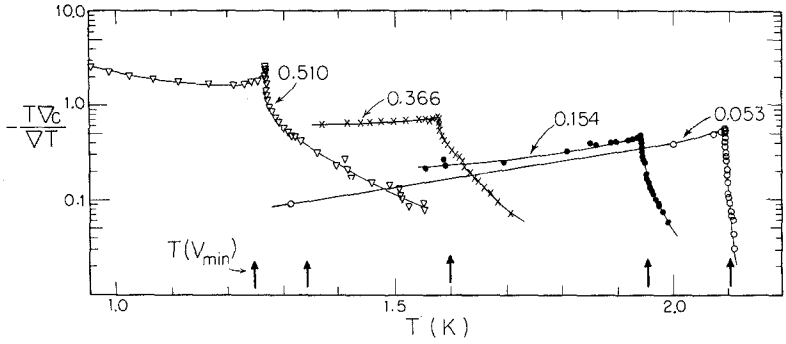


Fig. 5. Display of the data for $-T(\nabla c/\nabla T)$ versus T. In the normal phase this coefficient is the thermal diffusion ratio k_T. In the superfluid phase it is denoted by k_T^*.

investigated range, $0.1 \leqslant X \leqslant 0.3$. This is unexpected in view of the strong X dependence of the conductivity results.

Our basic measurements, just as those at Tokyo University,[16] determine grad V/grad T. As we have seen before, the factors $(\partial V/\partial T)_{X,P}$ and $(\partial X/\partial V)_{T,P}$ have singularities that become steeper as one approaches pure ^{4}He, and these are in opposite directions—sharp maximum and sharp minimum, respectively. When inserted in Eq. (13) these two singularities tend to cancel each other to a major extent, and qualitatively the final product k_T has the same shape as grad V/grad T. Interestingly, the sharp, lambda-like peak in k_T observed at higher ^{3}He concentrations disappears as X is decreased. In the superfluid phase the temperature profile of k_T becomes flat before the sharp decrease as the normal phase is entered. It is not excluded that our resolution at small ^{3}He concentrations, both in T and in X, becomes insufficient to observe a lambda-like sharp peak. We note that such a peak was reported by Ikushima,[19] but over a temperature range where we should have been perfectly able to detect it with the available resolution. The disappearance of the sharp peak in k_T at T_λ for $X \leqslant 0.37$ has been explained by Onuki (Ref. 33, Note added in proof).

In Fig. 5 we present a general view of the k_T data for mixtures studied in this laboratory. It is quite evident that there is an increase in the temperature dependence in the normal phase as X decreases, in contradiction with the Tokyo results. In Fig. 6 a logarithmic presentation on a reduced temperature scale shows the comparison with the results by Tanaka *et al.*[16] To a good approximation, these can all be represented by a single line. We also show the results by Lucas and Tyler for $X = 0.15$ that have recently been reanalyzed,[22] and where k_T was normalized to the value $k_T(T_\lambda) = 0.55$. It is quite evident that there is substantial disagreement among the results of the three groups.

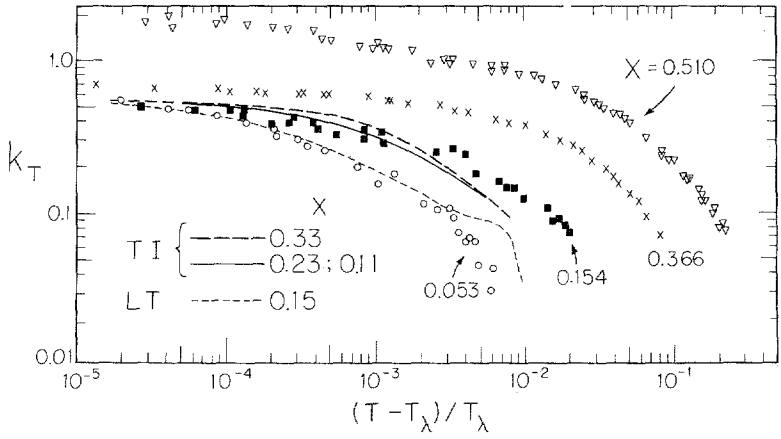


Fig. 6. The thermal diffusion ratio versus reduced temperature for four mixtures, and comparison with the data of Tanaka and Ikushima[17] (solid and heavy dashed lines TI) and those by Lucas and Tyler[15] (LT). The symbols denote the present data.

In the superfluid phase the predictions from Khalatnikov's theory, Eqs. (9)–(11), can be tested experimentally. In order to numerically evaluate Eq. (9) we use for $(\partial X/\partial\Delta)_{T,P}$ the values calculated for these same dilute mixtures by Ryschkewitsch and Meyer[23] from saturated vapor pressure and calorimetric data and for more concentrated mixtures[1] the values found from direct susceptibility data. Furthermore, we use the

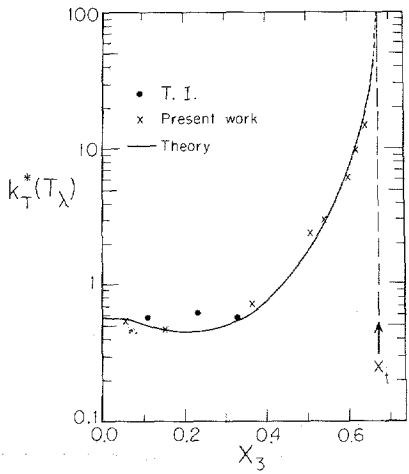


Fig. 7. The coefficient $k_T(\max)$ measured at the superfluid transition versus X, and comparison with the calculations using Eq. (3) based on the Khalatnikov theory.[11]

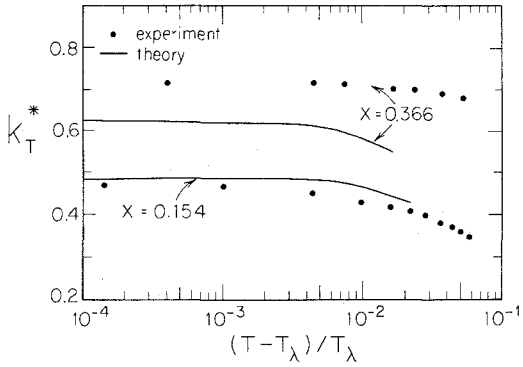


Fig. 8. The coefficient k_T^* in the superfluid phase versus the reduced temperature, and comparison with calculations using Eq. (3).

Fairbank–Buckingham relation

$$\left(\frac{\partial S}{\partial X}\right)_{P,T} \approx \left(\frac{dS}{dX}\right)_{\lambda,P} - \left(\frac{dT}{dX}\right)_{\lambda,P} \frac{C_{p,X}}{T} \tag{15}$$

together with the available derivative along the lambda line[12] and the calorimetric data in the superfluid phase.[24,25] Also, we obtain S/X from Ahlers' tabulation.[12] In Fig. 7 we show the value of $k_T^*(T_\lambda)$ calculated as a function of X and compared with our experimental data and those of Tanaka and Ikushima.[17,19] In the limit of very dilute mixtures the experimental results agree well with the predictions [Eq. (11)] and the observed shallow minimum in k_T^* is also in agreement with the predictions in Eq. (9). In Fig. 8 the temperature dependence for two dilute mixtures is shown. Given the different nature of the measurements used to calculate k_T^* via Eq. (4) and the fact that the determination of k_T^* from dielectric constant measurements also uses several thermodynamic parameters, we consider the agreement between theory and experiment extremely pleasing.

4. CHARACTERISTIC RELAXATION TIMES

These times were measured as described in detail in Ref. 26; the same apparatus was also used. Briefly, the experiment simultaneously measured the relaxation of the temperature and of the molar volume gradients versus time by means of the differential thermometer and capacitor top–bottom readings. Particularly for dilute ^{3}He–^{4}He mixtures, the time dependence of the molar volume is the sum of two terms including both the temperature

and concentration changes [see Eq. (12)]. The latter has the larger amplitude and longer decay time and therefore dominates. We obtained from two simultaneous recordings the time constants of the slowest modes giving $\tau(\nabla c)$ and $\tau(\nabla T)$, which describe the concentration and temperature gradient profiles with time. The results for the three dilute mixtures are shown in Fig. 9, where a sharp peak in both $\tau(\nabla c)$ and $\tau(\nabla T)$ is observed at the superfluid transition. Just as in more concentrated mixtures, both observed times are the same in the superfluid phase.

In the normal phase these times were analyzed in the same fashion as described before,[26] using the quantities obtained under stationary conditions

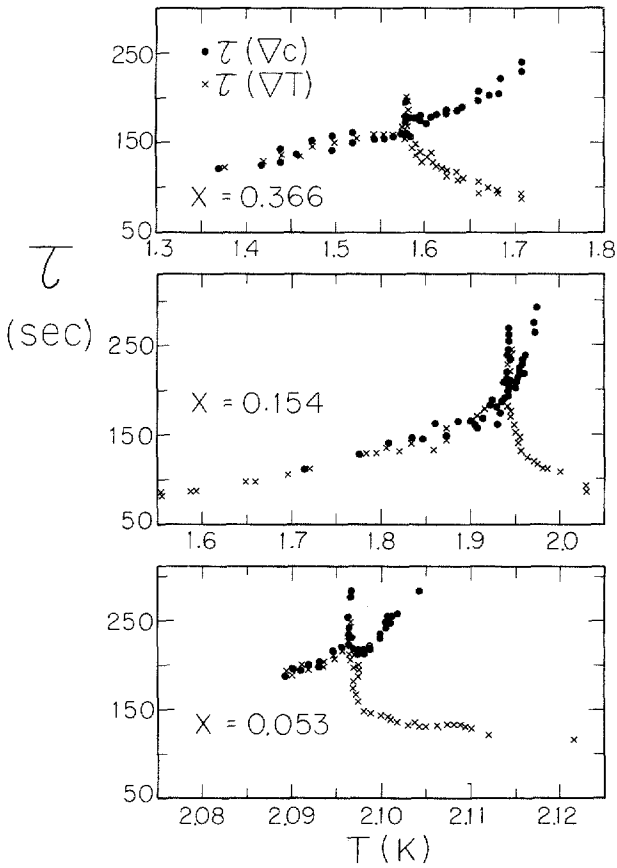


Fig. 9. Display of the measured relaxation times in three mixtures. $\tau(\nabla c)$ and $\tau(\nabla T)$ indicate the times for the concentration and temperature relaxation, respectively.

(κ and k_T) and various static properties [$C_{p,c}$, $(\partial c/\partial \mu)_{T,P}$] obtained from previous work.[23–25] Far enough above T_λ, where the coupling parameter $A = k_T^2 (\partial \mu/\partial c)_{T,P}/C_{p,c}T$ is much smaller than unity, the thermal and mass diffusion become uncoupled and the slowest characteristic times are, to a good approximation,

$$\tau(\nabla c) = D^{-1}(d/\pi)^2 \tag{16a}$$

$$\tau(\nabla T) = (\kappa/\rho C_{p,c})(2d/\pi)^2 \tag{16b}$$

In the superfluid phase the same analysis of the data was made as in Ref. 27. We now discuss successively the analysis in the two phases.

4.1. Normal Phase: The Mass Diffusion

The first measurements of the mass diffusion D for ^{3}He–^{4}He mixtures near the superfluid transition that investigated the predicted divergence[12] were those of Ahlers and Pobell.[28] These authors used a capacitive method to detect changes of the density with time after switching off the heat flux. These changes were measured under isothermal conditions, and the characteristic time constants were obtained. These are inversely proportional to D and hence a plot of τ versus the reduced temperature could demonstrate the divergence of D, which was the main purpose of the experiments. The absolute value of D was not reported, but an estimate was given using the expression $D = \tau^{-1} l^2$ with $l = 0.7$ cm the effective height of the cell. The difference with Eq. (16a) causes D to be too large by a factor of π^2.

Our own experiments differed from those of Ahlers and Pobell[28] in that the mixture was made to relax from one steady state with heat flux $q = 0$ to another with $q \neq 0$ or vice versa without the constriction of an isothermal process. We believed the boundary conditions to be better specified than in Ref. 28. Because numerical calculations of the coupling parameter A indicate substantial coupling between thermal and mass diffusion as T_λ is approached, we did not believe that a truly isothermal diffusion could take place.

To compare the results from the two approaches, we note first that the relaxation times observed by Ahlers and Pobell always decreased with the approach of T_λ and reached a nonzero value at T_λ that stayed constant in the superfluid phase. By contrast, our time $\tau(\nabla c)$ went through a minimum close to T_λ and then through a peak at the transition. The reason for this more complex behavior is that $\tau(\nabla c)$ is a function not only of D but also of several other parameters, as seen in the coupling parameter A that enters the hydrodynamic transport equations. The analysis of our results was therefore less straightforward than in the presumed isothermal situation.[28]

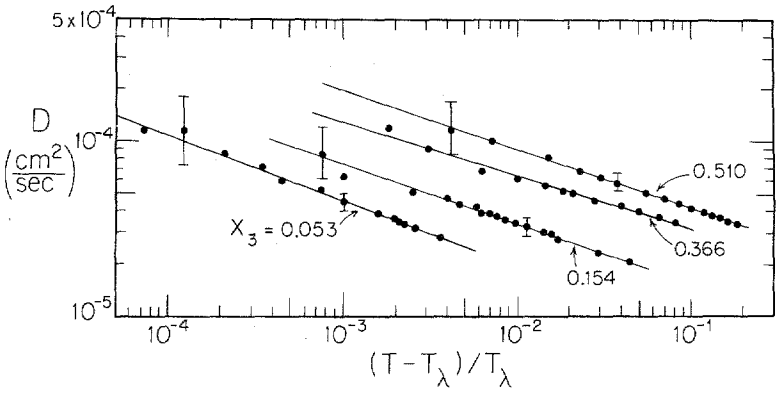


Fig. 10. The mass diffusion D versus reduced temperature for four mixtures.

In Fig. 10, where we present our results for D, we note that our analysis did not extend as close to T_λ as did that by Ahlers and Pobell, although our times were measured as close as $\varepsilon = 1 \times 10^{-5}$. The reason is as follows: As the parameter A increases with the approach of T_λ due to the sharp increase of k_T, the relaxation time $\tau(\nabla c)$ becomes increasingly dependent on A relative to D, and hence the determination of the latter from the solution of Eq. (15) in Ref. 26 becomes very insensitive. The errors on D have already been discussed in Ref. 26. In our Fig. 10 they have the same meaning, and represent an uncertainty of ± 5 sec in the measurement of τ and also of $\pm 10\%$ in the value of the coupling parameter A.

If the diffusion data obtained from the relaxation times of Ref. 28 are normalized at an arbitrary reduced temperature and a given X to interpolate between our results, then in the region of temperature overlap the agreement between the two sets of data is good, as shown in Fig. 11. Here D has been plotted versus X at several reduced temperatures, using both the results of Ref. 28 and our own. The effective length obtained from the normalization, using Eq. (16a) is then $l = 0.55$ cm, which is comparable with the dimensions used in Ref. 28. Hence, we conclude that the measurements by Ahlers and Pobell must have taken place under essentially isothermal conditions, but we still do not understand why this is so in view of the strong mass diffusion–thermal diffusion coupling.

We now briefly discuss the characteristic relaxation time $\tau(\nabla T)$. As described in detail in Ref. 26, the times $\tau(\nabla c)$ and $\tau(\nabla T)$ measure characteristic times of the slowest mode (mode 1) and the next slowest mode (mode 2), respectively, when thermal and mass diffusion motions are nearly uncoupled ($A \ll 1$). However, as the coupling increases with the approach

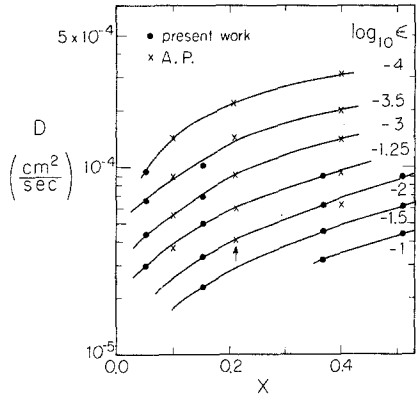


Fig. 11. The mass diffusion D versus X at several reduced temperatures and comparison with D inferred from the relaxation times τ of Ref. 28, and normalized to our data at the place marked by an arrow.

of T_λ, the ∇T transient terms reflect to an increasing degree the contribution of the slowest mode 1. Hence the measured $\tau(\nabla T)$ is in reality a weighted average over primarily the decay of modes 1 and 2. Sufficiently close to T_λ, when A is comparable with unity, the amplitude of mode 1 dominates and $\tau(\nabla T)$ tends to $\tau(\nabla c)$. This can be seen in Fig. 12, which illustrates the progressive importance of mode 1 with respect to mode 2 in the transient decay of ∇T for $X = 0.154$ at three representative temperatures. The amplitudes of the modes were calculated using the expressions of Ref. 26 together with the appropriate static and transport properties measured for this mixture. The resulting decay (sum over the two modes) is compared with the experimental one. We remind the reader that the experimental decay of the ∇T transients was not used in any of the analysis discussed before. It was exclusively the ∇c transient, where the amplitude of the slowest mode always dominates, that was used to determine the coefficient D.

Before concluding this section, we calculate the dispersion coefficients D_0 and D_2 for the two solutions to the coupled diffusion equations [Eqs. (3a) and (3b) of Ref. 26]. Denoting the two frequencies by Γ_0 and Γ_2 and the wave vector by q, one has

$$\Gamma_{0,2}/q^2 = D_{0,2} = \tfrac{1}{2}(D(1+A) + D_T \mp \{[D(1+A) + D_T]^2 - 4DD_T\}^{1/2}) \qquad (17)$$

where $D_T = \kappa/\rho C_{p,c}$. This equation is equivalent to Eq. (4.37) in Ref. 6 and to Eq. (15) of the paper by Griffin.[29] In the superfluid phase D_0 corresponds to a diffusive mode observed in the Rayleigh linewidth of the scattered light, while D_2 expresses the second-sound damping. We use the experimentally determined static and transport properties for the mixtures

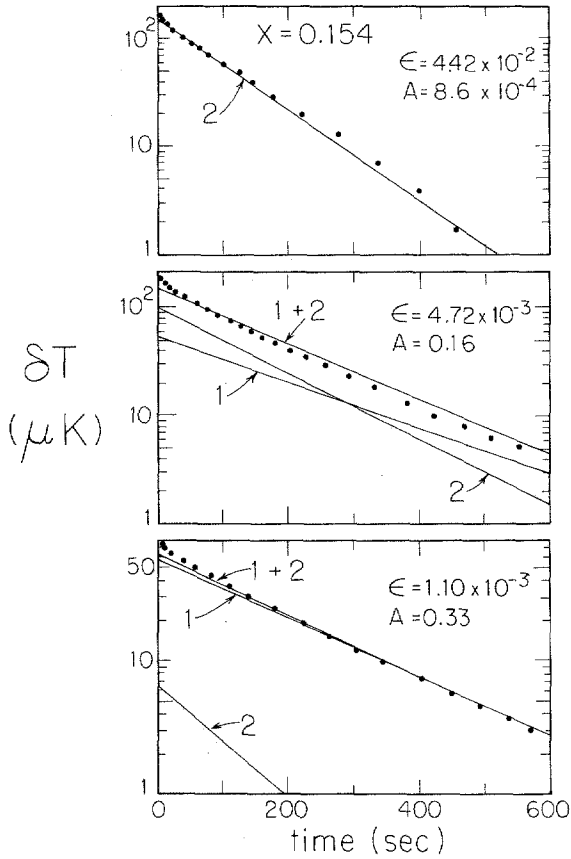


Fig. 12. The decay of the T transients with time for the mixture $X = 0.154$ at three temperatures, showing the contributions from the first two modes and their sum. As the coupling parameter A increases, the contribution of the slowest mode 1 becomes dominant.

(Refs. 23–25 and this research). In Fig. 13 we show D_0 and D_2 for the three diluted mixtures. In the limit of weak coupling between mass and thermal diffusivities ($A \approx 0$) the two solutions are

$$D_0 = D, \qquad D_2 = D_T \tag{18}$$

Hence, as T_λ is approached, D_0 increases, as to be expected from the behavior of the mass diffusion coefficient (Fig. 10). D_2 decreases at first because the specific heat increases faster than the thermal conductivity; it

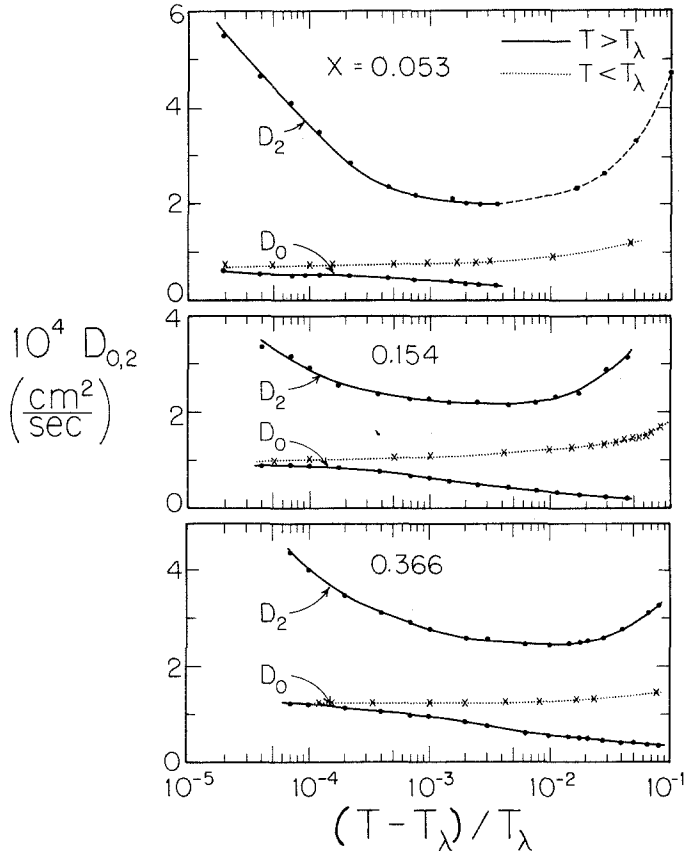


Fig. 13. The calculated solutions D_0 and D_2 of the coupled diffusive equations for three dilute mixtures as a function of reduced temperature in the normal and superfluid phases. Solid circles: $T > T_\lambda$; crosses: $T < T_\lambda$.

then passes through a minimum. For the mixtures $X = 0.053$ the measurements did not extend into the temperature range where this minimum is observable. However, using conductivity data for a similar mixture at a pressure slightly above saturated vapor pressure[13] taken in a different cryostat, we have calculated D_2 under the approximation $A = 0$. The results are shown by the dashed line, and are a smooth continuation of our data. For the $X = 0.053$ mixture, Dohm *et al.*[6] have calculated D_0 and D_2 using the same experimental data, and therefore both sets of curves agree. In addition, these authors have calculated the corresponding light scattering amplitudes and discussed in detail the resulting predicted structure factor. Tanaka and Ikushima[18] have calculated D_0 and D_2 for several mixtures,

using their results for k_T and the coefficient D deduced from the relaxation times of Ahlers and Pobell.[28] However, the amplitudes for D were incorrect. Furthermore, as we have seen before, there are systematic differences between the k_T data obtained by Tanaka and Ikushima[18] and by ourselves. As a result, there is a substantial discrepancy in the coefficients D_0 and D_2 between the work at Tokyo and Duke Universities. It can best be assessed by comparing Figs. 4 and 6 of Ref. 18 with our Fig. 13.

4.2. Superfluid Phase

As a result of the Khalatnikov hydrodynamic equations, the time constant τ for the slowest mode can be expressed[27] in terms of other measured quantities by means of a scaled relation

$$\tau/\tau^* = \psi(A^*) \tag{19}$$

where $\psi(A^*)$ is described by Eqs. (14)–(16) of Ref. 27, and where

$$\tau^* = d^2 \rho C_{p,c}/\kappa_{\text{eff}} \tag{20a}$$

$$A^* = (k_T^*)^2 (\partial\mu/\partial c)_{T,P}/TC_{p,c} \tag{20b}$$

The parameter A^* in the superfluid phase is the analog to A in the normal phase and expresses the coupling between thermal and mass diffusive motions.

In Fig. 14 we present the scaled plot, where we show by the solid line the predicted relation, Eq. (19), and by the various symbols the experimental results. Here we have used $(\partial\mu/\partial c)_{T,P}$ calculated in Ref. 23, the calorimetric data from Refs. 24, 25, 30, and 31, and the density, conductivity, and k_T^* data from the present work. For comparison, we have again added to the new results those for $X = 0.51$ reported before. For the latter, however, direct measurements of $(\partial\mu/\partial c)_{T,P}$ reported in Ref. 23 were used, together

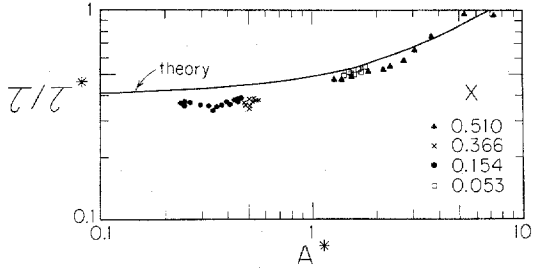


Fig. 14. The reduced relaxation time τ/τ^* versus the coupling parameter A^* for several mixtures as denoted by the different symbols. The solid line is the scaled function $\tau/\tau^* = \psi(A^*)$ for the slowest mode [Eq. (17)].

with the k_T^* and κ data of Ref. 1 and the calorimetric results from Ref. 30. The tendency[27] of the data to lie somewhat below the theoretical curve is continued by the more dilute mixtures as shown in Fig. 14. This discrepancy tends to be independent of A^* when A^* becomes small. This indicates that τ^* is too large by about 15%, reflecting a systematic error that most likely might be in the value of the effective path length d and in the thermal conductivity (itself determined using the path length). Certainly the reason for the discrepancy should be investigated by performing similar experiments with a different cell height. Figure 14 illustrates an interesting aspect of A^*, which for a given mixture is found to increase as T_λ is approached: This parameter is smallest for the $X = 0.15$ mixture, and hence, for more diluted mixtures, the coupling between mass and thermal diffusion increases again!

In summary, in spite of some problems, which could be caused by some systematic error in one or several of the quantities used to obtain A^* and τ^*, the reasonable consistency between theory and experiment is encouraging and should stimulate the investigation of still more dilute mixtures, where A^* becomes larger.

Finally, we calculate the dispersion relation for the diffusive branch Γ_0/q^2, where Γ_0 is the Rayleigh linewidth to be observed in light scattering experiments. From Griffin's equation (15) and using our Eqs. (3) and (5) from the Khalatnikov theory, we obtain

$$\Gamma_0/q^2 = D_0 = (\kappa_{\text{eff}}/\rho C_{p,c})(1+A^*)^{-1} \tag{21}$$

The crosses in Fig. 13 represent the diffusivity D_0 calculated from Eq. (21) using the experimental data mentioned before, and it can be seen that the results from the normal and the superfluid phases join smoothly at the phase transition. From the inspection of Eqs. (17) and (21), it cannot be predicted immediately that this should be so. It is to be hoped that light scattering measurements on the Rayleigh line will be carried out to test the predictions from these equations.

5. SUMMARY

We have presented measurements of several transport properties, namely the heat conductivity, the thermal diffusion ratio, and the mass diffusion, in diluted mixtures over a temperature range including the superfluid transition. Special emphasis was given to the study of the singular behavior of these properties near the transition. We have also calculated the Rayleigh linewidth for these mixtures expected in both the normal and the superfluid phases.

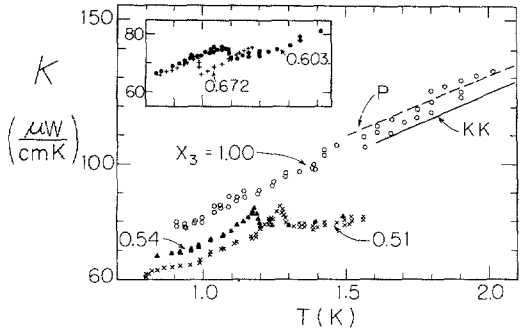


Fig. 15. Thermal conductivity of liquid ^{3}He at saturated vapor pressure (open circles) and comparison with the results of Kerrisk and Keller[34] (KK) and Pittman *et al.*[35] (P); and thermal conductivity of concentrated ^{3}He–^{4}He mixtures at saturated vapor pressure. To avoid overlap, the mixtures $X = 0.672$ and 0.603 are presented in the insert.

The results for the two most diluted mixtures have been discussed in detail by Dohm *et al.* in conjunction with their recent predictions.[6] After our paper was completed, we received a further theoretical paper by Onuki[32] on the critical transport properties of ^{3}He–^{4}He mixtures. Clearly there is considerable interest in dilute mixtures. At this stage, the easiest comparison between theory and experiments is for mixtures with $X < 0.1$ and we can use the numerical predictions[6] based on the $X = 0.05$ data to compare with still more dilute mixtures. Such experiments are now in progress in this laboratory.

APPENDIX A

In Ref. 1 a calculational mistake was made with a geometrical factor entering the calculation of the thermal conductivity in liquid ^{3}He–^{4}He mixtures and in ^{3}He. The evaluation of the conductivity data has been done again, and in Fig. 15 we present the results. For the case of ^{3}He, we can make the comparison with previous data by Kerrisk and Keller[33] and Pittman *et al.*[34] at the high-temperature end. Good agreement is obtained. At the low temperatures the data are smoothly continued by those of Anderson *et al.*[35] The good agreement with previous work indicates that the use of the nominal dimensions for our more complicated cell was justified. The necessity in using small heat fluxes in the ^{3}He measurements to avoid convection led to the large scatter in the data (for ^{3}He, $(\delta V/\delta T) > 0$).

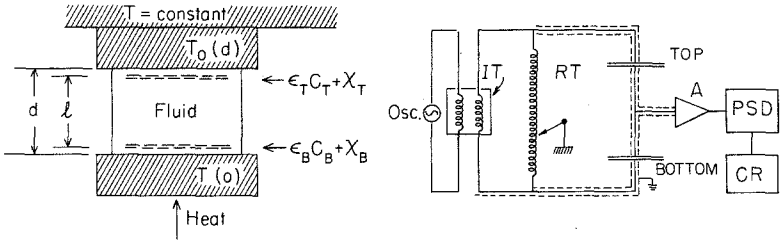


Fig. 16. Schematic presentation of the experimental cell and capacitor bridge. The symbols mean: IT, isolation transformer; RT, ratio transformer; A, amplifier; PSD, phase sensitive detector; CR, chart recorder.

APPENDIX B. MEASUREMENT OF THE DENSITY GRADIENT IN THE CELL

Our cell and the capacitance bridge arrangement are shown schematically in Fig. 16. The perforated capacitors (Buckbee-Mears Co., St. Paul, Minnesota, Micro-etch Stainless steel, part 5-1, 26% open area) are electrically connected to a seven-digit ratio transformer. Through reversal of a switch each of these capacitances can also be measured separately by means of a standard capacitor. Unlike in previous work,[23] space and thermal conductivity considerations did not permit the construction of a capacitor system with a shielding electric guard ring. Hence some stray capacitance was present, which, however, could be determined from the measurement of the total capacity at the top and bottom, with and without immersion in liquid helium of known density.

The ratio K read off the balanced ratio transformer system is then given by

$$R = \frac{\varepsilon_B C_B + \chi_B}{\varepsilon_B C_B + \chi_B + \varepsilon_T C_T + \chi_T} \tag{A1}$$

where ε is the dielectric constant, C is the capacitor immersed in the fluid, χ is the stray capacitance, and the subscripts B and T denote bottom and top. The temperature changes $\delta C/C$ and $\delta\chi/\chi$ are measured to be much smaller than the corresponding ones of $\delta\varepsilon/\varepsilon$. The ratio change δR for a temperature gradient in the cell then simplifies to

$$\frac{\delta R}{R(1-R)} \simeq \delta\varepsilon_B\left(1-\frac{\chi_B}{C_B}\right) - \delta\varepsilon_T\left(1-\frac{\chi_T}{C_T}\right) \tag{A2}$$

Measurements gave the values $\chi_B/C_B = 0.20 \pm 0.01$ and $\chi_T/C_T = 0.22 \pm 0.01$, and to simplify we assume them both to be equal to 0.21. Hence, finally,

$$\delta R/R(1-R) = (\delta\varepsilon_B - \delta\varepsilon_T)(1-0.21) = \delta\varepsilon_{BT}0.79 \tag{A3}$$

From the Clausius–Mossotti relation, the molar volume change $\delta V = V_B - V_T$ becomes

$$\delta V = -[4\pi\alpha/(\varepsilon-1)^2]\,\delta\varepsilon_{BT} \tag{A4}$$

Here α is the polarizability of helium, which is the same for both isotopes within experimental error.[36] Finally,

$$\frac{\text{grad } V}{\text{grad } T} = -\frac{\delta\varepsilon_{BT} r 4\pi\alpha}{\delta T_{BT}(\varepsilon-1)^2} \tag{A5}$$

where $r = d/l$ is the ratio of the distance between the copper plates to that between the centers of the superposed capacitors, and δT_{BT} is the temperature difference between bottom and top. In our experiment, $r = 1.29 \pm 0.02$, and we have assumed linear density and temperature changes with height. However, we have no way to check how well this assumption is realized. A rough estimate of possible systematic errors, mainly from geometry uncertainties, gives about $\pm 5\%$ for the measurement of grad V/grad T. The scatter in the data of $\delta\varepsilon$ was usually of the order of $\sim 5\%$ except close to T_λ, where the small temperature changes ($\delta T \approx 15\ \mu$K) necessitated by the singularity of k_T and κ caused scatter up to about $\pm 15\%$.

ACKNOWLEDGMENTS

One of the authors (HM) is greatly indebted to Drs. Dohm, Folk, and Bhattacharjee for very stimulating discussions and correspondence on the respective results in helium mixtures. The authors greatly appreciated the help and guidance of Dr. R. P. Behringer in the mathematical problems involved in obtaining the mass diffusion, and for many discussions. One of the authors (HM) is further indebted to Drs. Ahlers and Pobell for discussions related to their relaxation measurements. The authors also thank Dr. Ahlers for his comments on the manuscript.

REFERENCES

1. G. Ruppeiner, M. Ryschkewitsch, and H. Meyer, *J. Low Temp. Phys.* **41**, 179 (1980); H. Meyer, G. Ruppeiner, and M. Ryschkewitsch, in *Dynamical Critical Phenomena and Related Topics*, C. P. Enz, ed. (Springer, Berlin, 1979), p. 171.
2. D. Gestrich and H. Meyer, to be published; *Bull. Am. Phys. Soc.* **28**, 675 (1983); D. Gestrich, M. Dingus, and H. Meyer, *Physics Letters A*, to be published.
3. M. Papoular, *J. Low Temp. Phys.* **24**, 105 (1976).
4. K. Kawasaki and J. D. Gunton, *Phys. Rev. Lett.* **29**, 1661 (1972).
5. E. D. Siggia and D. R. Nelson, *Phys. Rev.* B **15**, 1427 (1977).
6. V. Dohm and R. Folk, *Phys. Rev.* **B28**, 1332 (1983).
7. J. Bhattacharjee, to be published.
8. V. Dohm and R. Folk, in *Advances in Solid State Physics*, P. Grosse, ed. (Vieweg, Braunschweig, 1982); *Physica* **109/110B**, 1549 (1982).

9. G. Ahlers, P. C. Hohenberg, and A. Kornblit, *Phys. Rev. B* **25**, 2136 (1982); P. C. Hohenberg, *Physica* **109/110B**, 1436 (1982).
10. E. D. Siggia, *Phys. Rev. B* **15**, 2830 (1977).
11. I. M. Khalatnikov, *Introduction to the Theory of Superfluidity* (Benjamin, New York, 1965), Section 24.
12. G. Ahlers, in *The Physics of Liquid and Solid Helium*, Part I, K. H. Bennemann and J. B. Ketterson, eds. (Wiley, New York, 1976).
13. L. H. Cohen, M. Dingus, and H. Meyer, to be published.
14. G. Ahlers, *Phys. Rev. Lett.* **24**, 1333 (1970).
15. P. Lucas and A. Tyler, *J. Low Temp. Phys.* **27**, 281 (1977).
16. M. Tanaka, A. Ikushima, and K. Kawasaki, *Phys. Lett.* **61A**, 119 (1977).
17. M. Tanaka and A. Ikushima, *Phys. Lett.* **64A** (1978).
18. M. Tanaka and A. Ikushima, *J. Low Temp. Phys.* **35**, 9 (1979).
19. A. Ikushima, *Jpn. J. Appl. Phys.* **19**, 2315 (1980).
20. H. Kierstead, *J. Low Temp. Phys.* **24**, 497 (1976).
21. A. Kakizaki and T. Sato, *J. Low Temp. Phys.* **24**, 67 (1976).
22. P. Lucas, private communication.
23. M. Ryschkewitsch and H. Meyer, *J. Low Temp. Phys.* **35**, 103 (1979).
24. F. M. Gasparini and M. R. Moldover, *Phys. Rev. B* **12**, 93 (1973).
25. T. Takada and T. Watanabe, *J. Low Temp. Phys.* **41**, 221 (1980).
26. R. P. Behringer and H. Meyer, *J. Low Temp. Phys.* **46**, 407 (1982).
27. R. P. Behringer and H. Meyer, *J. Low Temp. Phys.* **46**, 435 (1982).
28. G. Ahlers and F. Pobell, *Phys. Rev. Lett.* **32**, 144 (1974).
29. A. Griffin, *Can. J. Phys.* **47**, 429 (1969).
30. R. De Bruin-Ouboter, *Physica* **26**, 853 (1960).
31. T. A. Alvesalo, P. M. Berglund, S. T. Islander, G. R. Pickett, and W. Zimmermann, Jr., *Phys. Rev. A* **4**, 2354 (1971).
32. A. Onuki, *J. Low Temp. Phys.* **53**, 189 (1983).
33. J. F. Kerrisk and W. E. Keller, *Phys. Rev.* **177**, 341 (1969).
34. C. E. Pittman, L. H. Cohen, and H. Meyer, *J. Low Temp. Phys.* **46**, 115 (1982).
35. A. C. Anderson, J. I. Connolly, O. E. Vilches, and J. C. Wheatley, *Phys. Rev.* **147**, 86 (1966).
36. E. C. Kerr and R. H. Sherman, *J. Low Temp. Phys.* **3**, 451 (1970).